J Toxicol Pathol 2023; 36: 187–192

Case Report

Histopathology of fused triplet placenta in rat

Satoshi Furukawa[1*], Naho Tsuji[2], Seigo Hayashi[3], Yusuke Kuroda[3], Masayuki Kimura[3], Chisato Kojima[3], and Kazuya Takeuchi[3]

[1] Planning and Development Department, Nissan Chemical Corporation, 2-5-1 Nihonbashi, Chuo-ku, Tokyo 103-6119, Japan
[2] Planning and Development, Agricultural Chemical Division, Nissan Chemical Corporation, 2-5-1 Nihonbashi, Chuo-ku, Tokyo 103-6119, Japan
[3] Biological Research Laboratories, Nissan Chemical Corporation, 1470 Shiraoka, Shiraoka-shi, Saitama 349-0294, Japan

Abstract: A fused triplet placenta was observed in a Wistar Hannover rat on gestation day 15. Each placenta (referred to as PL-A, PL-B, and PL-C) of this fused placenta was attached to one fetus each, but their fetal weights were lower than that of the fetus attached to the only normal placenta (referred to as PL-N) in this dam. Histopathologically, thinning of the trophoblastic septa and dilatation of the maternal sinusoid in the labyrinth zone were observed in PL-B and PL-C, but not in PL-A or PL-N. The points of placental fusion were at the junctional zone derived from each side of the placenta without connective tissues, and the septum was composed of trophoblastic giant cells. Although PL-A had a solitary metrial gland, PL-B and PL-C shared one metrial gland with one spiral artery terminus branching towards each labyrinth zone. (DOI: 10.1293/tox.2023-0026; J Toxicol Pathol 2023; 36: 187–192)

Key words: fused placenta, metrial gland, rat, spiral artery, triplet

In humans, multiple pregnancies related to placental fusion are an important problem in perinatal care because of the high perinatal mortality rate, sequelae of prematurity, and fetal intrauterine growth restriction (IUGR)[1]. Fused placentas have been known to occur in humans[2], pigs[3], cattle[4], rabbits[5], and rodents[6, 7]. It has been reported that the incidence of a fused placenta is 1% of normal pregnancies in mice[8, 9]. However, the mechanisms underlying placental fusion and the effects of placental fusion on placental exchange and endocrine function remain unknown[10]. In rats, a fused placenta is not exceedingly uncommon, and there are a few case reports on histopathological changes in the fetal part (labyrinth and junctional zones)[11] of the fused placenta[6, 7, 12]. However, there have been no reports of morphological changes in the maternal part (decidua basalis and metrial gland)[11] of the fused placenta in rats or mice. In this study, we encountered a fused triplet placenta in a rat, and described its detailed histopathological morphology.

This animal was a pregnant specific pathogen-free (SPF) Wistar Hannover rat (BrlHan:WIST@Jcl(GALAS), CLEA Japan, Tokyo, Japan), purchased at 11 weeks of age. The animal was one of the rats supplied for a bisphenol A oral gavage perinatal study: this study consisted of the control and bisphenol A groups exposed at a dose of 300 mg/kg from gestation day (GD) 6 to 20, and 4–5 dams per group were sampled each time on GDs 13, 15, 17, and 21. GD 0 was designated as the day on which the vaginal plug was identified. The animals were single-housed in a plastic cage on softwood chip bedding in an air-conditioned room (22 ± 2°C; 55 ± 10% humidity; 12 h/day light cycle). Food (CRF-1; Oriental Yeast Co., Ltd., Tokyo, Japan) and water were provided ad libitum. This animal was euthanized by exsanguination under anesthesia with isoflurane, and necropsied on GD 15. All fetuses were removed from the placentas and weighed. The fetal and placental samples were fixed in 10% neutral-buffered formalin. This study was conducted according to the Guidelines for Animal Experimentation, Biological Research Laboratory, Nissan Chemical Corporation, and the Statement about sedation, anesthesia, and euthanasia in a rodent fetus and newborn (2015) of the Japanese College of Laboratory Animal Medicine.

The placentas were embedded in paraffin blocks, and 4-µm thick sections were stained with routine hematoxylin and eosin (HE) stain, Masson's trichrome stain, and periodic acid-Schiff (PAS) stain. Sections were subjected to immunohistochemical staining of phospho-histone H3 (Ser10; Cell Signaling Technology, Boston, MA, USA) for mitotic activity evaluation[13]. The following parameters were measured in the sections per placenta using an image analyzer (WinROOF, Mitani Co., Tokyo, Japan): the area of each part of the placenta close to the central portion of the placenta by HE staining and the number of phospho-histone H3-positive

Received: 24 February 2023, Accepted: 11 May 2023
Published online in J-STAGE: 5 June 2023
*Corresponding author: S Furukawa
(e-mail: furukawa@nissanchem.co.jp)

cells in 20 sections of each part per placenta with a 40× objective. In addition, the area ratio of the maternal sinusoid in the labyrinth zone was measured in five sections per placenta with a 20× objective using an all-in-one fluorescence microscope (BZ-X810, Keyence Co., Osaka, Japan). The means and standard deviations of the area ratio of the maternal sinusoid in the labyrinth zone were calculated (Pharmaco Basic, Scientist Press Co., Ltd., Tokyo, Japan). For comparisons among the placentas, the Dunnett's multiple comparison test was performed after the Bartlett's test. The level of significance was set at $p<0.05$ and <0.01.

Macroscopically, the animal had one implantation site and one fused triplet placenta (referred to as PL-A, PL-B, and PL-C) with three fetuses in the right uterine horn, and one placental remnant and one normal placenta (referred to as PL-N) with one fetus in the left uterine horn (Fig. 1). These implantations were closely adjacent to each other in each area on both sides of the uterine horn. Each fetus attached to the fused triplet placenta had its own umbilical cord. The weights of these fetuses were lower than that of the fetus attached to PL-N (Table 1). In particular, the weights of the fetuses attached to PL-B and PL-C were lower than the one attached to PL-A. However, the fetal weights in this dam were heavier than the means of fetal weight in dams in the control (0.250 ± 0.033 g, 4 dams, 42 fetuses) and bisphenol A (0.260 ± 0.032 g, 4 dams, 50 fetuses) groups in the bisphenol A oral gavage perinatal study (Table 1). The increased fetal weights in this dam were attributed to the low number of fetuses, and these fetuses were not considered to be strictly IUGR. In addition, this fused placenta was thought to be spontaneous and not induced by bisphenol A treatment because there was only one dam with a fused placenta among the 17 dams exposed to bisphenol A. To our knowledge, there are no reports of fused placentas caused by bisphenol A in rats[14].

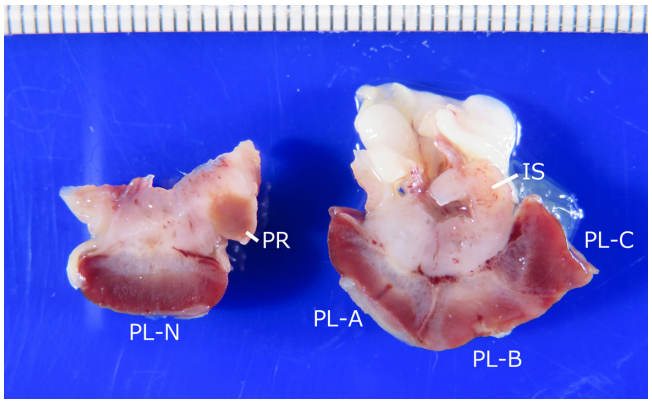

Fig. 1. Gross appearance of normal placenta (PL-N) on left and fused triplet placenta (PL-A, PL-B, and PL-C) on right. Note the placental remnant (PR) associated with normal placenta and single uterine implantation site (IS) close to fused placenta.

Histopathologically, the fetal part of the normal placenta was oval-shaped in PL-N, whereas that of the fused triplet placenta was fan-shaped in PL-A, and heart-shaped in PL-B and PL-C (Fig. 2). In the labyrinth zone, there was thinning of the trophoblastic septa caused by decreased cellular components (atrophy) and dilatation of the maternal sinusoid in PL-B and PL-C, but not in PL-A and PL-N. There was a significantly increased area ratio of the maternal sinusoid in the labyrinth zone in PL-B and PL-C (Fig. 3). No vascular anastomoses were observed between the labyrinth zones of the fused placentas. In the junctional zone, glycogen cell islands were formed in the fused placentas as in PL-N; thus, it was considered that there was apparently no growth retardation in this part of the fused triplet placenta (Fig. 2). The points of placental fusion were at the junctional zones derived from each side of the placenta, and the areas of junctional zone fusion were composed of trophoblastic giant cells without connective tissues (Fig. 4a). In the metrial gland, PL-A had a solitary metrial gland, but angioectasia of the spiral artery terminus ran off-center (Figs. 2, 4b). The metrial gland of PL-A was separated from that of PL-B and PL-C by poor connective tissue components (Figs. 2, 4c); the boundary showed reduced vascularization and increased PAS stain-positive u-NK cell infiltration. Both PL-B and PL-C shared one decidua basalis and one metrial gland, and one spiral

Table 1. Fetal Weight and Histological Analysis of Fused Placenta

		Fused			Normal
		PL-A	PL-B	PL-C	PL-N
Fetal weight (g)		0.337	0.294	0.273	0.392
Area of each part of placenta (mm^2)	Labyrinth zone	15.2	7.3	14.09	19.4
	Junctional zone	10.9	15.4	12.15	13.8
	Decidua basalis	1.3	5.3	Sharing/PL-B	2.9
	Metrial gland	16.4	11.8	Sharing/PL-B	16.6
No. of histone H3 positive cells (20 areas/placenta ×40)	Labyrinth zone	45	39	39	44
	Junctional zone	0	0	0	0
	Decidua basalis	0	0	Sharing/PL-B	0
	Metrial gland	19	23	Sharing/PL-B	17

Fetal weights in for a bisphenol A oral gavage perinatal study.
- Control group, 0.250 ± 0.033 g (4 dams, 42 fetuses).
- Bisphenol A-treated group, 0.260 ± 0.032 g (4 dams, 50 fetuses).

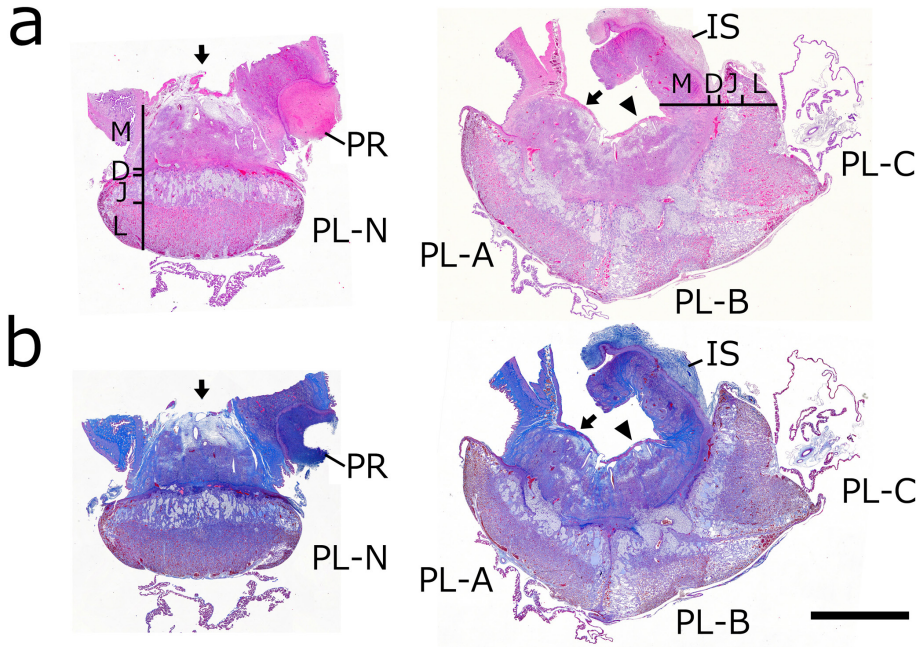

Fig. 2. Low magnification images of normal (left) and fused (right) placentas stained with either hematoxylin and eosin (a) or Masson's trichrome (b). Solitary metrial gland for PL-N and PL-A (arrow) and shared metrial gland of PL-B/PL-C (arrowhead). Boundary consisting of poor connective tissue components between metrial gland of PL-A and shared one of PL-B/PL-C, whereas the boundary consisting of abundant connective tissue between shared one of PL-B/PL-C and implantation site. Bar, 4,000 μm; D, decidua basalis; IS: implantation site; J: junctional zone; L: labyrinth zone; M: metrial gland; PR: placental remnant.

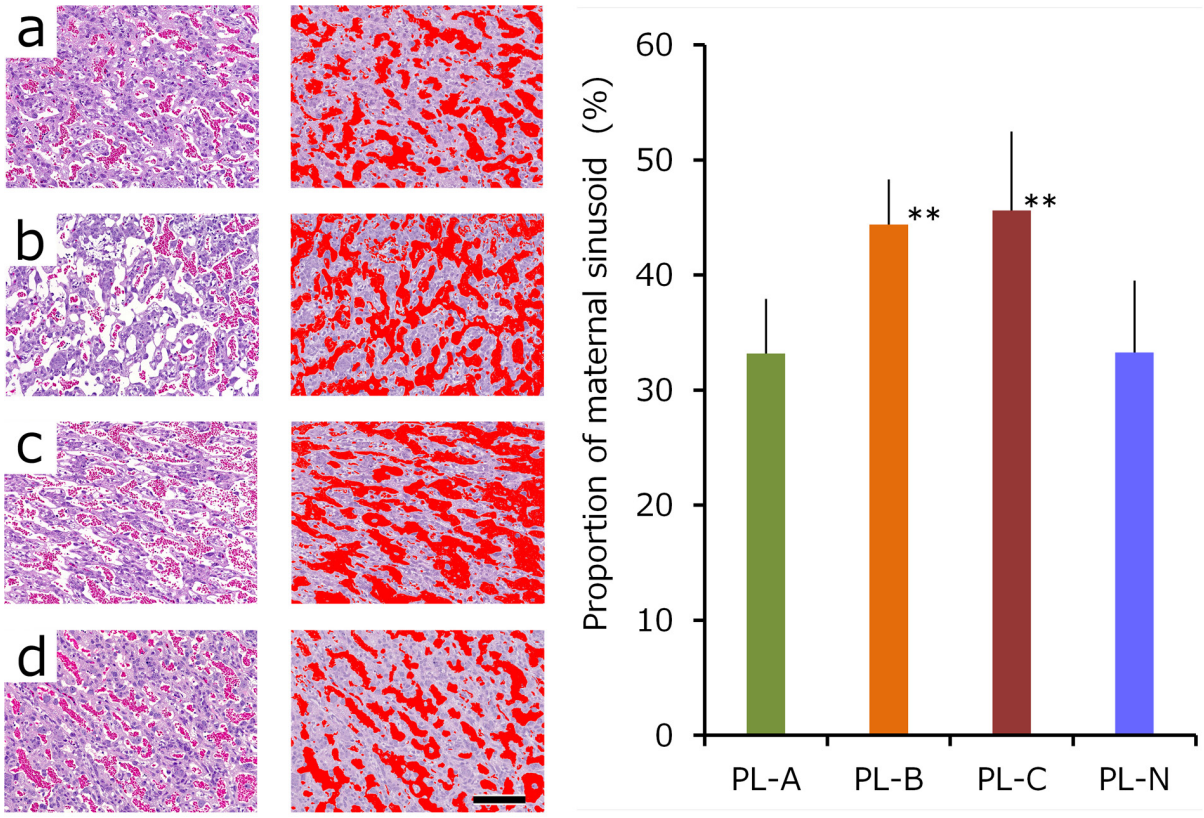

Fig. 3. Histopathology and area ratio of maternal sinusoid in labyrinth zone. Thinning of trophoblastic septa and significantly increased area ratio of maternal sinusoid in PL-B and PL-C. Left, hematoxylin and eosin stain; Right, imaging of maternal sinusoid. a, PL-A; b, PL-B; c, PL-C; d, PL-N. Bar, 150 μm. Each value represents mean ± standard deviation. **Significantly different from control at $p<0.01$ (Dunnett's test).

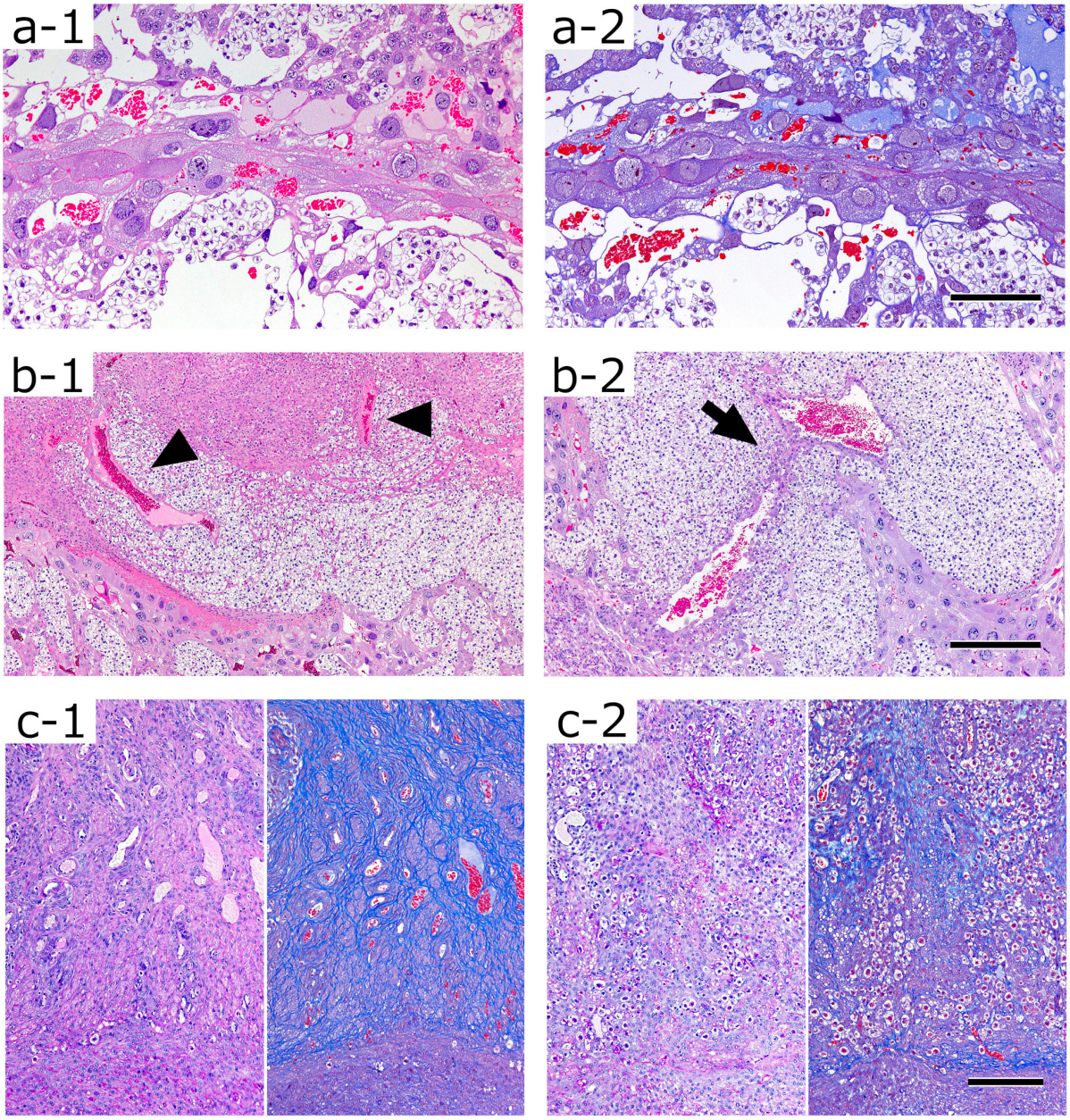

Fig. 4. Histopathology in fused placenta. a. Histopathological change of point of placental fusion. Areas of junctional zone fusion in PL-A and PL-B composed of trophoblastic giant cells. Masson's trichrome staining illustrates lack of connective tissue at this site. 1, Hematoxylin and eosin (HE) stain; 2, Masson's trichrome stain. Bar, 200 µm. b. Histopathological change of spiral artery terminus. Angioectasia of spiral artery terminus (arrowhead) in PL-A. Spiral artery terminus branched (arrow) towards each labyrinth zone of PL-B and PL-C. 1, PL-A; 2, PL-B/PL-C. HE stain. Bar, 500 µm. c. Histopathological changes at metrial gland boundaries. Panel on the left (c-1) shows a clear boundary between implantation site and PL-B/PL-C metrial gland regions, owing to the abundant connective tissue. Panel on the right (c-2) shows an unclear boundary between the PL-A and PL-B/PL-C metrial gland regions, with less connective tissue and reduced vascularization compared to c-1. Left, periodic acid-Schiff stain; Right, Masson's trichrome stain. Bar, 200 µm.

artery terminus branched at the metrial gland towards each labyrinth zone of PL-B and PL-C (Figs. 2, 4b). This shared metrial gland was clearly separated from the adjacent implantation site by the connective tissue (Figs. 2, 4c). There were no differences in cell proliferative activity in each part between the placentas in this dam (Table 1). The areas of the labyrinth zone of PL-A, PL-B, and PL-C and the shared metrial gland of PL-B and PL-C were markedly smaller than that of PL-N (Table 1).

In the present case, the three umbilical cords leading to the individual fetuses had their own placenta of the fused triplet placenta separated from each other. It may be appropriate to classify this fused triplet placenta macroscopically as a separate triamnionic trichorionic placenta, according

to the type of placentation in humans[2, 15]. However, the three placentas of the fused triplet placenta were in contact with each other at the junctional zone; such a change has been reported in previous studies on fused placentas in rodents[12, 16, 17]. In addition, the two placentas of the fused triplet placenta shared one metrial gland, which is the first time that such a change has been reported in rodents. These morphological changes are anatomically unique to rodents; thus, it is difficult to classify this case according to the type of human placentation.

In this dam, the weights of fetuses attached to the fused triplet placenta were lower than that of the fetus attached to the normal placenta. Reduced fetal weights are expected with fused placentas, which could be attributed to a relative reduction in maternal-fetal exchange areas due to the small-sized labyrinth zone. In particular, the markedly low fetal weights of PL-B and PL-C were probably due to reduced maternal blood flow to each labyrinth zone caused by the sharing of a metrial gland. In addition, atrophy of the trophoblastic septa and a dilated maternal sinusoid in the labyrinth zones were observed in these placentas, but not in PL-A. Thus, these lesions in the labyrinth zone may be closely related to circulatory disturbances via reduced maternal blood flow.

In polytocous species, including rodents[18, 19], a number of fertilized eggs enter the uterine horn, followed by embryo implantation in an evenly distributed pattern along the longitudinal uterine axis, which is referred to as 'embryo spacing'. Experimentally, placental fusion is induced by superovulation or the transfer of fertilized eggs into the uterus in mice, resulting from the limited available intrauterine space[9]. In addition, the disruption of embryo spacing is induced by the inhibition of myometrial contractile activity by relaxin, adrenergic drugs, and prostaglandin synthesis inhibitors in mice[20]. Genetically, uneven embryo spacing has been observed in engineered mouse models, such as Pla2g4a(−/−) mice deficient in cytosolic phospholipase A2a and Lpar3(−/−) mice deficient in the third receptor for lysophosphatidic acid[21]. In the present case, the number of implantations was low and the implantations, including the fused triplet placenta, were concentrated in one area in each of the respective uterine horn. Furthermore, despite the separation of the fetal parts of the triplet placenta, the metrial glands are shared or had indistinct boundaries. Although the cause is unknown, it is speculated that fertilized eggs were specifically implanted without sufficient spacing in the dam, resulting in a fused triplet placenta.

Collectively, the histopathological changes and developmental mechanisms of placental fusion in rats are not necessarily identical to those in humans. Further detailed investigations, including the histological evaluation of placental pathology in rat-fused placentas, are necessary to compare the histology and physiology of rat and human placental fusion.

Disclosure of Potential Conflicts of Interest: The authors declare no conflicts of interest.

Acknowledgement: The authors thank Ms. Yukiko Sudo, Ms. Kaori Maejima, Ms. Hiromi Asako, Mr. Atsushi Funakoshi, Mr. Makoto Tsuchiya, and Mr. Yoshinori Tanaka for their excellent technical assistance.

References

1. Breathnach FM, and Malone FD. Fetal growth disorders in twin gestations. Semin Perinatol. **36**: 175–181. 2012. [Medline] [CrossRef]
2. Chan JSY. Multiple pregnancies. In: Benirschke's Pathology of the Human Placenta, 7th ed. RN Baergen, GJ Burton, and CG Kaplan (eds). Springer, Cham. 413–505. 2022.
3. Sudha R. Morphology and morphometric study of placenta and umbilical cord with its vascular pattern and comparative anatomy. 2009, from Upgraded Institute of Anatomy Madras Medical College & Research Institute website: http://repository-tnmgrmu.ac.in/228/1/202300109sudha.pdf
4. López-Gatius F. Response to therapeutic abortion in lactating dairy cows carrying dead twins during the late embryo/early fetal period. Animals (Basel). **11**: 2508. 2021. [Medline] [CrossRef]
5. Bomsel-Helmreich O, and Papiernik-Berkhauer E. Delayed ovulation and monozygotic twinning. Acta Genet Med Gemellol (Roma). **25**: 73–76. 1976. [Medline] [CrossRef]
6. Carr JG. Further observations on placental fusion in mice, and a report of a case in the rat. Proc R Soc Edinb Biol. **62**: 304–306. 1947. [Medline]
7. Hofmann T, Schneider S, Wolterbeek A, van de Sandt H, Landsiedel R, and van Ravenzwaay B. Prenatal toxicity of synthetic amorphous silica nanomaterial in rats. Reprod Toxicol. **56**: 141–146. 2015. [Medline] [CrossRef]
8. De Clercq K, Persoons E, Napso T, Luyten C, Parac-Vogt TN, Sferruzzi-Perri AN, Kerckhofs G, and Vriens J. High-resolution contrast-enhanced microCT reveals the true three-dimensional morphology of the murine placenta. Proc Natl Acad Sci USA. **116**: 13927–13936. 2019. [Medline] [CrossRef]
9. McLaren A, and Michie D. Experimental studies on placental fusion in mice. J Exp Zool. **141**: 47–73. 1959. [CrossRef]
10. Lopez-Tello J, and Sferruzzi-Perri AN. Fused placentas: till birth do us part. Placenta. **103**: 177–179. 2021. [Medline] [CrossRef]
11. Furukawa S, Tsuji N, and Sugiyama A. Morphology and physiology of rat placenta for toxicological evaluation. J Toxicol Pathol. **32**: 1–17. 2019. [Medline] [CrossRef]
12. Arora KL. A case of placental fusion in a Sprague Dawley rat. Lab Anim Sci. **27**: 377–379. 1977. [Medline]
13. Moroki T, Matsuo S, Hatakeyama H, Hayashi S, Matsumoto I, Suzuki S, Kotera T, Kumagai K, and Ozaki K. Databases for technical aspects of immunohistochemistry: 2021 update. J Toxicol Pathol. **34**: 161–180. 2021. [Medline] [CrossRef]
14. Kim JC, Shin HC, Cha SW, Koh WS, Chung MK, and Han SS. Evaluation of developmental toxicity in rats exposed to the environmental estrogen bisphenol A during pregnancy. Life Sci. **69**: 2611–2625. 2001. [Medline] [CrossRef]
15. Pharoah POD. Causal hypothesis for some congenital anomalies. Twin Res Hum Genet. **8**: 543–550. 2005. [Medline] [CrossRef]

16. Ladman AJ. Histological observations on placental apposition in mice. Anat Rec. **125**: 41–53. 1956. [Medline] [CrossRef]
17. Elmore SA, Cochran RZ, Bolon B, Lubeck B, Mahler B, Sabio D, and Ward JM. Histology atlas of the developing mouse placenta. Toxicol Pathol. **50**: 60–117. 2022. [Medline] [CrossRef]
18. O'Grady JE, and Heald PJ. The position and spacing of implantation sites in the uterus of the rat during early pregnancy. J Reprod Fertil. **20**: 407–412. 1969. [Medline] [CrossRef]
19. Restall BJ, and Bindon BM. The timing and variation of pre-implantation events in the mouse. J Reprod Fertil. **24**: 423–426. 1971. [Medline] [CrossRef]
20. Chen Q, Zhang Y, Elad D, Jaffa AJ, Cao Y, Ye X, and Duan E. Navigating the site for embryo implantation: biomechanical and molecular regulation of intrauterine embryo distribution. Mol Aspects Med. **34**: 1024–1042. 2013. [Medline] [CrossRef]
21. Ye X, Hama K, Contos JJ, Anliker B, Inoue A, Skinner MK, Suzuki H, Amano T, Kennedy G, Arai H, Aoki J, and Chun J. LPA3-mediated lysophosphatidic acid signalling in embryo implantation and spacing. Nature. **435**: 104–108. 2005. [Medline] [CrossRef]